Nucl Med Mol Imaging (2015) 49:200–207
DOI 10.1007/s13139-015-0336-2

ORIGINAL ARTICLE

ISSN (Online) 1869-3482
ISSN (Print) 1869-3474

Synthesis and Evaluation of ^{99m}Tc-Labeled Folate-Tripeptide Conjugate as a Folate Receptor-Targeted Imaging Agent in a Tumor-Bearing Mouse Model

Myoung Hyoun Kim[1] · Woo Hyoung Kim[2] · Chang Guhn Kim[1,3] · Dae-Weung Kim[1,3]

Received: 3 February 2015 / Revised: 8 April 2015 / Accepted: 12 April 2015 / Published online: 8 May 2015

Abstract
Purpose The folate receptor (FR) is an attractive molecular target since it is overexpressed in a variety of human tumors. The purpose of the present study was to synthesize and evaluate the feasibility of a novel ^{99m}Tc-ECG-EDA (Glu-Cys-Gly-ethylenediamine)-folate as an FR-positive tumor imaging agent in a mouse tumor model.
Materials and Methods ECG-EDA-folate was synthesized using solid phase peptide synthesis (SPPS) and radiolabeled with ^{99m}Tc using tripeptide ECG as a chelator. FR-positive KB cells were inoculated in athymic nude mice. Following injection of ^{99m}Tc-ECG-EDA-folate, serial scintigraphy and micro-SPECT/CT imaging were performed at various time points with and without pre-administration of excess free folate. Mean count densities (MCD) for regions of interest drawn on KB tumors and major normal organs at each time point were measured, and uptake ratios of tumor to normal organs were calculated.
Results ECG-EDA-folate was labeled with ^{99m}Tc with high radiolabeling efficiency and stability (>96 %). FR-positive tumors were clearly visualized on both scintigraphy and micro-SPECT/CT images and the tumor uptake of ^{99m}Tc-ECG-EDA-folate was markedly suppressed with faint visualization of tumors by pre-administration of excess free folate on serial planar scintigraphy, indicating FR-specific binding of the agent. Furthermore, semiquantitative analysis of MCD data showed again that both tumor MCD and tumor-to-normal organ ratios decreased considerably by pre-administration of excess free folate, supporting FR-specific tumor uptake. Tumor-to-normal organ ratios approximately increased with time after injection until 4 h.
Conclusion The present study demonstrated that ^{99m}Tc-ECG-EDA-folate can bind specifically to FR with clear visualization of FR-positive tumors in a mouse tumor model.

Keywords Folate receptor · Molecular imaging · Technetium 99m · SPECT

Introduction

The folate receptor (FR) is an attractive molecular marker for diagnostic radionuclide imaging. The FR is overexpressed in a variety of human cancers, but its expression is highly limited in normal tissues [1]. Folate, a water-soluble and essential vitamin B complex, works as a coenzyme for the biosynthesis of nucleotides and amino acid metabolism [2]. Thus, folate has an important role in the development and proliferation of cells.

Folate has several advantages as a molecular targeting ligand, such as its small molecular weight (441.4 g/mol), non-immunogenic property, stability under the harsh chemical conditions required for radiolabeling procedures, and finally a high affinity for FR even after labeling with radionuclides [3].

Manuscript has not been published before or is not under consideration for publication anywhere else and has been approved by all co-authors.

✉ Chang Guhn Kim
leokim@wonkwang.ac.kr

[1] Department of Nuclear Medicine, Wonkwang University School of Medicine, Iksan, Korea

[2] Department of Nuclear Medicine, Seoul National University Hospital, Seoul, Korea

[3] Institute of Wonkwang Medical Science, Iksan, Korea

FR expression has been shown to correlate with tumor differentiation and to be a prognostic factor in some cancers [2, 4]. Therefore, whole-body radionuclide imaging using FR-targeted radiolabeled folate can serve as a useful tool to evaluate the FR expression status of tumor in patients. The favorable properties of folate and FR described above have been exploited to develop a variety of radiolabeled folate as an imaging agent, including ^{67}Ga-deferoxamine-folate, ^{111}In-DTPA-folate, ^{99m}Tc-ethylenedicysteine-folate, ^{99m}Tc-HYNIC-folate, ^{99m}Tc-DTPA-folate, ^{99m}Tc-EC20, and ^{99m}Tc/^{188}Re-PAMA-folate [3, 5, 6]. ^{99m}Tc-EC20, among others, is the most successful radiolabeled folate in clinical trials [3]. It is conjugated with short peptides (Cys-Asp-Dap-D-Glu) as chelators and shows a high tumor uptake [6, 7].

Short peptides (oligopeptide) have increasingly gained attention as bifunctional chelating ligands for metallic radionuclides owing to their versatile functionality to conjugate with a variety of biomolecules [8]. Interestingly, however, use of folate receptor-targeted ligands based on peptides as chelating agents for ^{99m}Tc is highly limited [5, 6].

Herein, this preliminary study was aimed to synthesize and evaluate the feasibility of a novel ^{99m}Tc-Glu-Cys-Gly-ethylenediamine (ECG-EDA)-folate as an FR-targeted molecular imaging agent in mice bearing FR-positive KB tumors.

Materials and Methods

All chemical compounds and reagents including folic acid dihydrate, amino acid, $SnCl_2$ dihydrate, sodium tartrate dibasic dihydrate, and HCl were obtained from appropriate commercial companies. ^{99m}Tc-pertechnetate was eluted from a commercial technetium generator (Elumatic III, CIS BIO International, France). Athymic nude mice (BALB/c nu/nu, weighing 16–18 g) were purchased from the Daehan Biolink, Co. Ltd (Seoul, Korea). Folate-free animal chow (TD.95247, Teklad) was purchased from the Harlan Laboratories Inc. (Indianapolis, IN, USA). KB cells, a human squamous carcinoma cell line, was purchased from the Korean Cell Line Bank (Seoul, Korea).

Synthesis of ECG-EDA-folate

Tripeptide (Glu-Cys-Gly, ECG) was chosen as a ^{99m}Tc chelating ligand and ethylenediamine (EDA) was used as a linker between ECG and the carboxyl group of glutamate residue of folic acid. ECG-EDA-folate was synthesized using solid-phase peptide synthesis (SPPS) and obtained from AnyGen Corp. (Gwangju, Korea). Briefly, EDA was attached to trityl resin and sequential conjugation of BocNH-ECG-COOH was done. Thereafter, BocNH-ECG-EDA was conjugated with folic acid and purified. The synthesized compound was analyzed by high performance liquid chromatography (HPLC) on a Shimadzu C18 analytical column (C18, 5 μm, 100 Å column, 4.6×250 mm) and the mass was analyzed by MS spectrometry (AXIMA-CFR, MALDI-TOF Mass Spectrometer). Although ECG-EDA-folate contains a mixture of α- and γ-folate (EDA conjugated with a α- or γ-carboxylate residue of folate, respectively), the chemical structure is predominantly ECG-EDA-γ-folate (>95 %), as shown in Fig. 1.

Radiolabeling of ^{99m}Tc-ECG-EDA-folate

The ligand exchange method was employed by using tartrate as a co-ligand. In a 3-ml reaction vial, 0.1 mg of ECG-EDA-folate, 25 μl of tartrate solution (10 mg/25 μl in nitrogen-purged water), and 20 μl of $SnCl_2$ dihydrate solution were added (1 mg/ml in 0.01 M HCl solution). In a lead shielded fume hood, about 1850 MBq (50 mCi) of freshly eluted ^{99m}Tc-pertechnetate was added, and the reaction vial was heated in water bath for 30 min at 100 °C and cooled to room temperature.

Radiolabeling efficiency and stability was determined using instant thin layer chromatography–silica gel (ITLC-SG) with water (R_f of ^{99m}Tc-ECG-EDA-folate and free pertechnetate=0.9–1.0; R_f of colloid=0.0–0.1) and acetone (R_f of free pertechnetate=0.9–1.0; R_f of colloid and ^{99m}Tc-ECG-EDA-folate=0.0–0.1) as the mobile phases. Radiolabeling efficiency and stability was determined by radio-ITLC at 1, 2,, 4 and 8 h after incubation in human serum at 37 °C.

Mouse Tumor Model

The KB cells were maintained at 37 °C in a humidified atmosphere containing 5 % CO_2. Six-week-old female nude mice were kept in cages and fed tap water, and every mouse had free access to food and water. Because the normal rodent diet contains a high level of folate, mice were on a folate-free diet

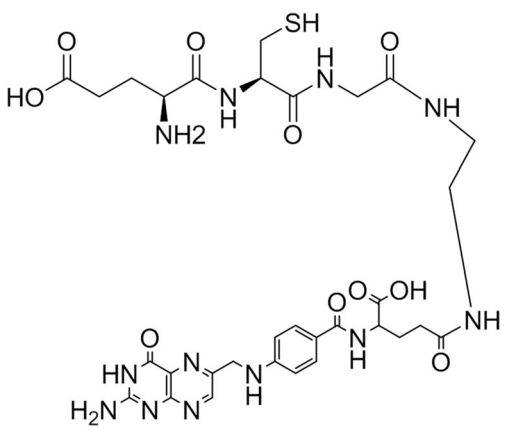

Fig. 1 Chemical structure of ECG-EDA-γ-folate

for at least 3 weeks to reduce serum folate to the physiologic level of humans, as previously reported [9]. After 3 weeks of the folate-free diet, KB cells (1×10^6 cells in 0.1 ml sterile PBS) were inoculated subcutaneously into the left axilla of each mouse. Growth of the tumors was measured in two perpendicular directions using a caliper, and the volumes of the tumors were calculated as $0.5\times L\times W^2$. Imaging studies were performed after tail vein injection of radiolabeled compound 7–10 days after tumor cell inoculation, when the longest diameters of tumors reached 10 mm.

Serial Planar Scintigraphy and Micro-SPECT/CT Imaging in Mice Bearing KB Tumor

After intravenous injection of 59.2–111 MBq of ^{99m}Tc-ECG-EDA-folate into the tail veins of KB tumor-bearing mice (n=2), serial static imaging was performed using dual head SPECT camera (Forte, Philips Medical Systems) with 3 mm pinhole collimator and window setting of 140 keV±20 %. Serial images were acquired at 30 min, 1, 2, and 4 h after injection. The static images were stored in a 256×256 matrix size and 500–1000 k counts were acquired. In addition, micro-SPECT/CT imaging was also performed in another mouse bearing a KB tumor at 22 h after intraperitoneal injection of 59.2 MBq of ^{99m}Tc-ECG-EDA-folate. Micro-SPECT/CT image was acquired with NanoSPECT/CT (Bioscan, Inc. USA). Scan parameters were as follows: multi-pinhole collimator; window setting of 20 % width at energy of 140 keV; 10 s per frame; 12° angular step collimator rotation. Images were reconstructed with nine iterations using ordered subset expectation maximization reconstruction algorithm.

In Vivo Competition (Inhibition) Study in Mice Bearing KB Tumor

To evaluate whether ^{99m}Tc-ECG-EDA-folate can specifically bind to FRs and compete with free folate, an in vivo binding inhibition (competition) study was performed. Before injection of ^{99m}Tc-ECG-EDA-folate, 0.125 mg of free folate (280 nM, about 20–25 times the concentration of ^{99m}Tc-ECG-EDA-folate) was administered via the tail vein of mice (n=3). Then serial imaging was done using the same procedure described above at 30 min, 1, 2, and 4 h after injection of ^{99m}Tc-ECG-EDA-folate.

Evaluation of Biodistribution Pattern Using Mean Count Density (MCD) Measurement

The traditional biodistribution study for ^{99m}Tc-ECG-EDA-folate was not performed in this study. Instead, a simple image analysis method using a ROI technique for measuring MCD (not total counts within the ROI, but average counts per pixel within the ROI) in organs or tissues was applied to evaluate biodistribution pattern approximately. On all images obtained from both in vivo competition and baseline serial imaging studies at each time point, ROIs were drawn over the KB tumor of the left axilla, muscle of thigh, mediastinum, and liver to measure MCD. Because the injected dose of radiotracer, image acquisition starting time (e.g., at 1 or 2 h), and acquisition time or duration (e.g., 30 s or 70 s) may differ among mice, actually measured MCDs should be standardized by adjusting the above factors in order to compare these data for further analysis. For example, when the actually measured MCD, averaged over three measurements for the liver obtained at 1 h after injection of 55.5 MBq radiotracer for 30 s acquisition time is 100 counts/pixel, then this is normalized to 37.0 MBq injected dose, 1 min acquisition time, and corrected for 1 h decay time. Normalized MCD can be calculated as follows: normalized MCD for the liver of mouse equals 100×37.0 MBq /55.5 MBq×60 s/30 s×1/0.891. In this study, however, MCD was used as complementary data to provide supportive, semiquantitative information for qualitative interpretation (visual inspection) of imaging results.

Tumor-to-non-target-tissue ratios were calculated using these MCD data, and the results of in vivo competition study were compared with those of the serial imaging study (baseline).

Statistical Analysis

Quantitative variables were expressed as mean±SD. The non-parametric Mann–Whitney U test was applied for independent samples of serial imaging and in vivo competition studies. P<0.05 was considered significant. The data were analyzed by SPSS version 18.0 (SPSS Inc., IBM Co.).

Results

Chemical purity analyzed by HPLC was 95.4 % (Fig. 2). The expected mass of ECG-EDA-folate ($C_{31}H_{40}N_{12}O_{10}S_1$) was 772.8 Da and measured mass by MS spectrometry was 773.6 Da. Radiolabeling efficiency and stability of ^{99m}Tc-ECG-EDA-folate determined by radio-ITLC at 1, 2, 4, and 8 h after incubation in human serum at 37 °C were 98.0, 98.0, 97.4, and 94.6 %, respectively (Fig. 3).

In serial scintigraphy of the mouse tumor model, the KB tumor in the left axilla was clearly visualized between 1 h and 4 h after injection, and the uptake intensity of the KB tumor gradually increased and reached a maximum at 4 h (Fig. 4a). On micro-SPECT/CT images at 22 h after intraperitoneal injection of the agent, the KB tumor was also clearly visualized (Fig. 5).

In competition study by pre-administration of excess free folate into tail veins of three mice, the uptake of radiolabeled

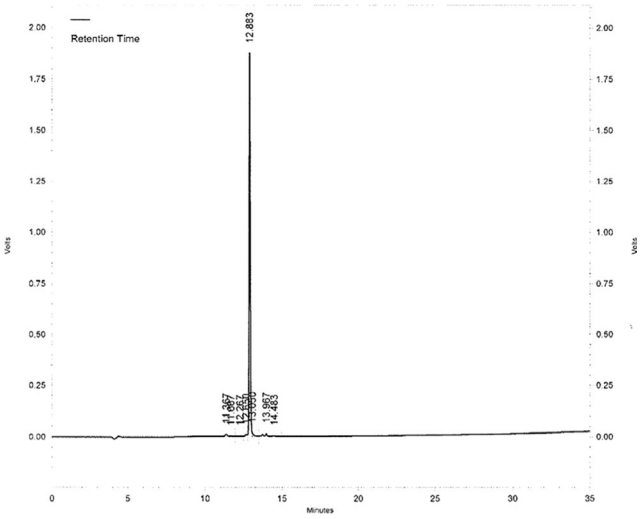

Fig. 2 HPLC of ^{99m}Tc-ECG-EDA-folate displayed a main single peak indicative of ECG-EDA-γ-folate (>95 %)

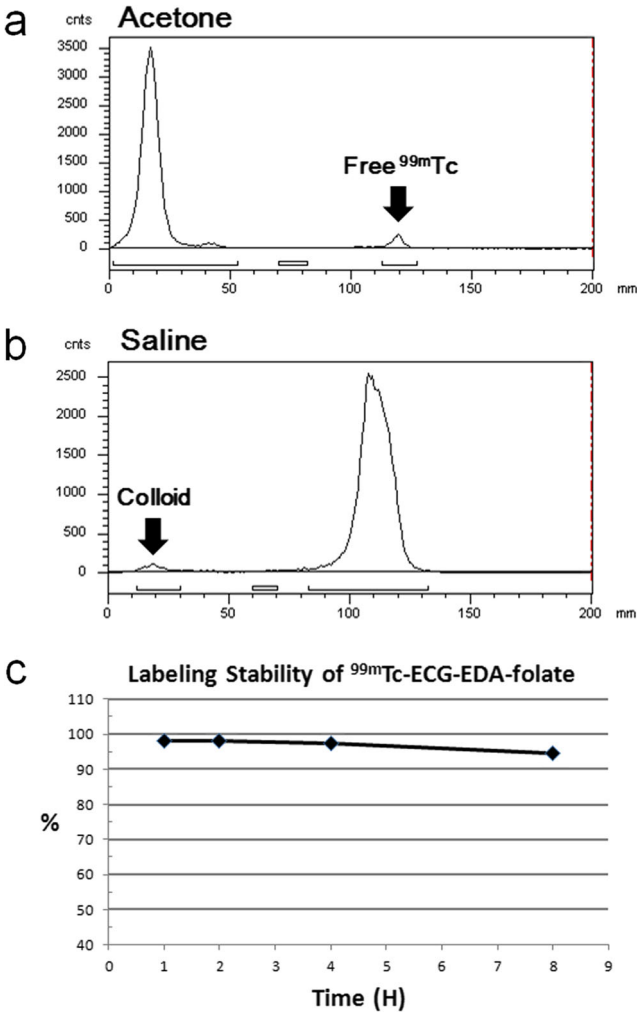

Fig. 3 **a**, **b** Representative radio-ITLC of ^{99m}Tc-ECG-EDA-folate at 8 h after incubation in human serum at 37 °C developed in acetone and saline as a mobile phase, respectively. **c** Radiolabeling stability up to 8 h in human serum at 37 °C

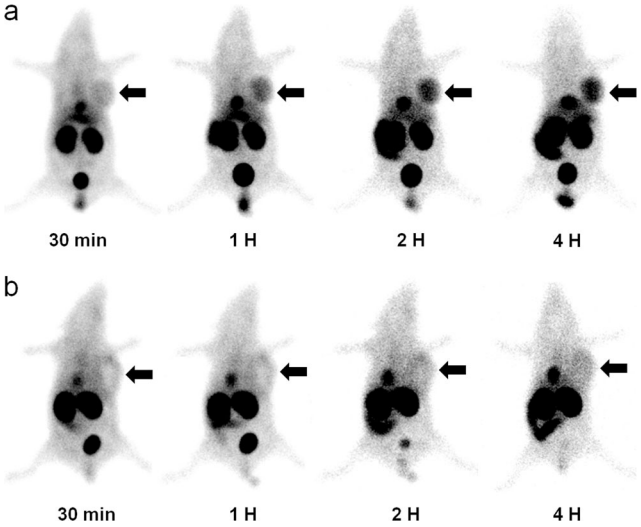

Fig. 4 **a** Representative serial scintigraphy of KB tumor-bearing mouse after administration of ^{99m}Tc-ECG-EDA-folate. FR-positive KB tumor in the left axilla is clearly visualized at 1, 2, and 4 h after injection. **b** Representative serial scintigraphy of KB tumor-bearing mouse after administration of ^{99m}Tc-ECG-EDA-folate with pre-administration of excess free folate (inhibition). Tumor uptake is markedly suppressed at 1, 2, and 4 h after injection. *Arrows* indicate FR-positive KB tumor

folate in FR-positive KB tumors was markedly suppressed and faintly visualized in comparison with those of baseline study, indicating FR-specific tumor uptake (Fig. 4b).

Semiquantitative evaluation of the biodistribution profile using MCD data (Table 1) showed again that both MCD of KB tumors and tumor-to-normal-organ ratios decreased considerably by intravenous pre-administration of excess free folate at all observation time points, supporting FR-specific binding of the agent (Figs. 6 and 7). However, the differences between competition and baseline study were not significant statistically ($p>0.08$) probably due to small sample size ($n=2$ and 3, respectively). Tumor-to-non-target-tissue uptake ratios approximately increased with time after injection of the agent until 4 h (Fig. 7).

Among non-target normal organs, the liver, gall bladder, intestine, and kidneys showed the most intense uptake during early phase after injection, and the uptake intensity persisted with time.

Discussion

Folate receptor-targeted imaging has been studied exploiting the mechanism by which folate can enter cells. There are three major mechanisms of folate entry into cells: reduced folate carrier (RFC) [10], proton-coupled folate transporter (PCFT) [11], and the high affinity FRs [12]. RFC presents ubiquitously in normal cells and has a high affinity for reduced folate such as tetrahydrofolate (THF). RFC also has a high affinity for antifolates, but a low affinity for folate [13].

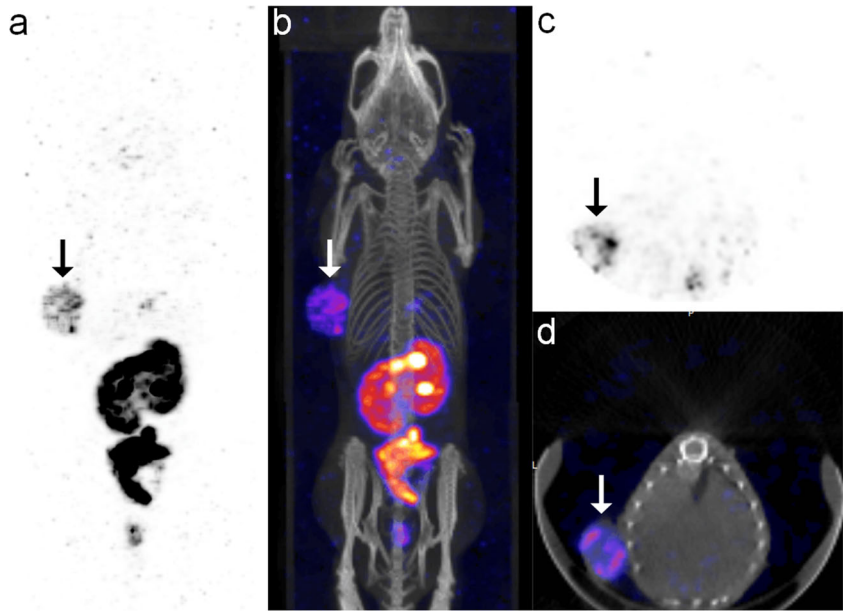

Fig. 5 Micro-SPECT/CT images of KB tumor-bearing mouse obtained at 22 h after intraperitoneal administration of ^{99m}Tc-ECG-EDA-folate. **a**, **b** MIP and fusion images show clear visualization of an FR-positive KB tumor in the left axilla (*arrows*). **c**, **d** Transaxial and fusion images of the KB tumor show rim-shaped tumor uptake with central photon defect

FR binds preferentially to folate. FR also shows a high affinity for folate conjugates, but a low affinity for reduced folate and antifolates [4, 14]. Thus, when a folate conjugate such as ECG-EDA-folate is injected intravenously, FRs in tumors bind preferentially to the folate conjugate than do RFCs in normal tissues. On the other hand, when excess free folate is administered intravenously, FRs in tumors can preferentially be saturated, leading to suppressed uptake of ECG-EDA-folate. In addition, when an antifolate such as pemetrexed is injected, RFCs in kidneys are preferentially affected, resulting in reduced renal uptake.

Table 1 Mean count densities of FR-positive KB tumor and non-target organs measured on serial scintigraphy after injection of ^{99m}Tc-ECG-EDA-folate with or without pre-administration of excess free folate

Organ	Time after injection	MCD* (mean±SD)		*P* value†
		in vivo imaging study (*n*=2)	in vivo inhibition study (*n*=3)	
KB tumor	30 min	3.93±0.82	2.77±0.52	0.248
	1 h	3.82±0.50	2.31±0.73	0.083
	2 h	3.52±0.17	2.06±0.66	0.083
	4 h	3.12±0.06	1.56±0.51	0.083
Muscle	30 min	1.03±0.05	1.04±0.26	0.564
	1 h	0.62±0.10	0.66±0.23	0.767
	2 h	0.46±0.04	0.48±0.19	0.767
	4 h	0.23±0.02	0.34±0.16	0.564
Blood	30 min	4.39±0.25	4.16±0.99	0.767
	1 h	2.62±0.21	3.01±1.29	0.564
	2 h	1.92±0.11	2.01±0.94	1.000
	4 h	1.35±0.10	1.41±0.62	0.564
Liver	30 min	6.04±0.93	4.63±1.24	0.564
	1 h	4.81±0.72	3.63±1.46	0.248
	2 h	3.64±0.27	2.89±1.11	0.564
	4 h	3.02±0.10	2.48±0.83	0.767

* decay corrected, normalized by injection dose and acquisition time (counts/pixel per 37 MBq of injection dose and 1 min acquisition time)

† *P* values of Mann–Whitney *U* test

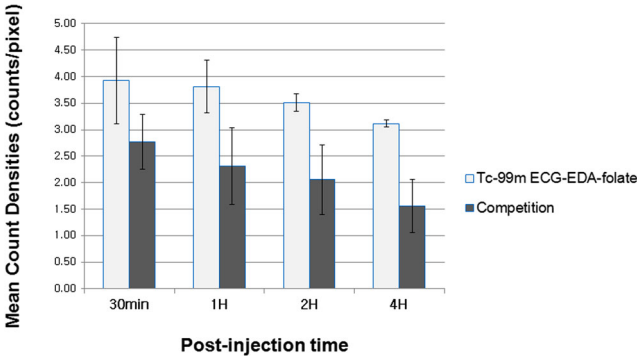

Fig. 6 Semiquantitative comparison of KB tumor uptake after injection of ^{99m}Tc-ECG-EDA-folate with or without pre-administration of excess free folate. MCDs of KB tumor in inhibition study decrease considerably in compared with those of baseline study. Data show mean count densities (counts/pixel) of KB tumors measured on gamma camera images, which are decay corrected and normalized by injected dose and acquisition time

At least three isoforms of FRs have been identified as FR-α, -β, and -γ. Expression of either FR-α or FR-β is highly restricted to the kidney, lung, placenta, and choroid plexus [1]. Importantly, FR-α is present in a variety of malignancies, including tumors of the ovary, endometrium, colon, lung, and breast. Finally, FR-β is seen mainly in activated macrophages and myeloid leukemic cells [4, 15].

ECG-EDA-folate was synthesized using all physiologic L-amino acids based on reported observations that the peptide used

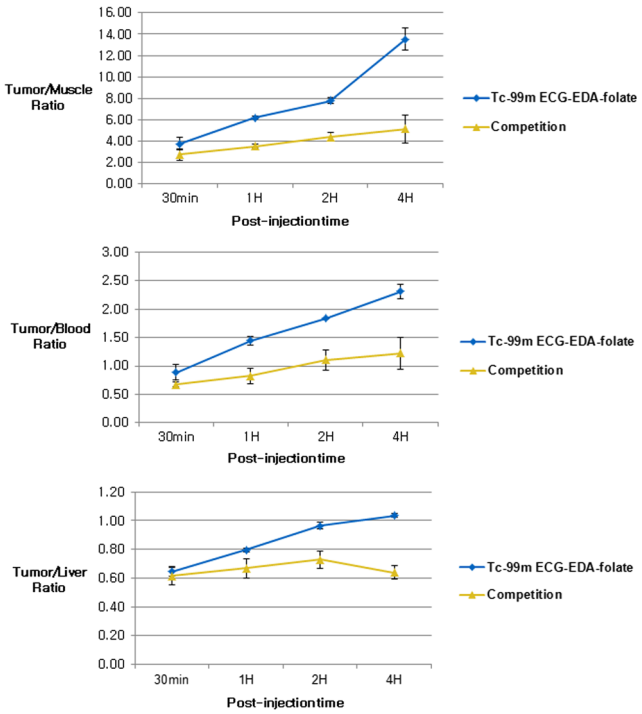

Fig. 7 KB tumor-to-non-target-organ ratios at 30 min, 1, 2, and 4 h after administration of ^{99m}Tc-ECG-EDA-folate with or without pre-administration of excess free folate. KB tumor-to-normal-tissue ratios in inhibition study decrease considerably in comparison with those of baseline study

in the synthesis of ^{99m}Tc-EC20 contained unphysiologic D-Glu, and substitution with all D-amino acids in this radiolabeled folate was shown to be clearly inferior to the original one [16].

During the synthetic process of ECG-EDA-folate using SPPS, EDA may conjugate with either α- or γ-carboxylate residues of folate, resulting in the presence of both chemical conformations in synthesized compounds. ECG-EDA-γ-folate was estimated to be more than 95 % as determined by HPLC (Fig. 2). It has been demonstrated that both α- and γ-folate can bind FRs specifically [17]. Thus, ECG-EDA-folate was used as received without further purification in this study.

Early after injection of ^{99m}Tc-ECG-EDA-folate, FR-positive KB tumors were excellently visualized, and the tumor radioactivity was markedly suppressed when excess free folate was pre-administered intravenously, indicating FR-specific binding of ^{99m}Tc-ECG-EDA-folate (Fig. 4). FR-specific tumor uptake was further supported by semiquantitative analysis of tumor MCD data and tumor-to-normal-organ ratios, which decreased considerably when excess free folate was pre-administered in comparison with those of baseline study (Figs. 6 and 7).

MCD (average counts per pixel within an ROI) measured from planar scintigraphy is based on summation of counts originating from overlapping organs or tissues within the ROI, not from single tissue (e.g., liver, kidney), whereas MCD (counts per voxel) obtained from SPECT images is determined by counts from specific organ or tissue. Thus, voxel-based MCD could be more reliable than pixel-based MCD. The advantage of using MCD (either pixel- or voxel-based) as complementary data for an approximate estimate of biodistribution is that it can be measured in an identical mouse at each imaging time point in an identical manner without need for sacrificing mice at each time point.

All the imaging findings clearly demonstrated that ^{99m}Tc-ECG-EDA-folate can specifically bind to FR-positive tumors, and its accumulation can persist for a prolonged period of time after injection of a radiotracer, which was the main focus of the present study, and again, MCD data were used only as complementary in the present study to semiquantitatively support the qualitative interpretation of imaging findings mentioned above.

On micro-SPECT/CT images obtained at 22 h after injection, a KB tumor was also clearly visualized, suggesting that this radiolabeled folate could accumulate in KB tumors for a substantial period of time.

When excess free folate is injected intravenously, FRs in KB tumors preferentially bind to free folate because of their higher affinity than RFC in normal tissues, resulting in more efficient suppression of uptake in KB tumors.

Unfavorably, substantial accumulation of radioactivity was observed in the gall bladder and bowel early after injection and increased gradually over time, suggesting rapid hepatobiliary excretion into the gall bladder and intestine, probably attributable, in part, to the hydrophobic nature of this radiolabeled folate.

Among normal tissues and organs, the kidney showed the highest radioactivity resulting from FR expression in the proximal tubule and reabsorption of radiolabeled folate in urine. These observations are common features of most radiolabeled folate reported so far. Detecting small FR-positive tumors in the abdominal cavity could be hampered by unfavorable accumulation of radioactivity in the intestine.

With regard to the high renal uptake of small molecular weight radiolabeled folate including ^{99m}Tc-ECG-EDA-folate, it could be explained by the fact that FRs in the apical (luminal) surface of proximal tubular cells, which are not accessible to blood vessels, reabsorb essential vitamin folate present in primitive urine. This is evidenced by observations that macromolecules or nanoparticles larger than 40 kDa or 5.5 nm in hydrodynamic diameter do not undergo glomerular filtration, leading to reduced renal uptake [18].

To improve hydrophilicity and enhance renal excretion of peptide-based radiolabeled folate, an approach that uses a peptide consisting of highly water-soluble amino acids may need to be further investigated. To overcome this problem, a small dose of free folate is injected before radiolabeled folate administration to partially saturate FRs in normal organs in clinical trials [7, 19]. An alternative to reduce renal uptake, an antifolate such as pemetrexed has been used to reduce renal uptake without significant change in tumor uptake [19]. Another approach is the use of an inhibitor of organic anion transporters that has been shown to block hepatic uptake [7].

Because biodistribution data were not available for ^{99m}Tc-ECG-EDA-folate, and the mouse tumor model (KB tumor in this study) was different from that used for ^{99m}Tc-EC20 (syngeneic FR-positive M109 tumor) [6], direct comparison between two radiolabeled folates using %ID/g was not possible. Another cited radiolabeled folate, ^{99m}Tc-EDA-ethylenedicysteine-folate (^{99m}Tc-EC-folate), was one of the first ^{99m}Tc-labeled folate conjugates containing dicysteine (EC) as a chelator [5]. They reported only <0.2 %ID/g in breast tumors (the 13762 cell line) of Fisher 344 rats at 4 h after injection of the radiotracer, in which the poor tumor uptake is possibly attributed, in part, to the low level of FR expression in this tumor cell line.

The limitations of the present study were that a small sample size was used in the baseline imaging study and a substantial accumulation of ^{99m}Tc-ECG-EDA-folate was observed in tumors following pre-administration of excess free folate, which was evident by MCD data shown in Table 1 and Fig. 6. This observation may raise argument on FR-specific uptake of this radiolabeled folate. In this regard, it may be possible to explain that radiochemical impurities, among other reasons, could, in part, contribute to nonspecific uptake of this radiolabeled folate. To resolve this problem, further investigations including radio-HPLC analysis and traditional biodistribution study may be needed.

Conclusion

The present study demonstrated that ^{99m}Tc-ECG-EDA-folate exhibits FR-specific, high tumor uptake in a tumor-bearing mouse model. The results of the current study could be useful for future study in design and development of folate peptide conjugate for FR-targeted imaging of tumor.

Acknowledgments This study was supported by Wonkwang University in 2013.

Conflict of Interest Myoung Hyoun Kim, Woo Hyoung Kim, Chang Guhn Kim, and Dae-Weung Kim declare that they have no conflict of interest.

Ethical Standard All procedures performed in this study involving animals were approved by the animal ethics committee in our university and were in accordance with the ethical standards laid down in the 1964 Declaration of Helsinki and its later amendments.

References

1. Parker N, Turk MJ, Westrick E, Lewis JD, Low PS, Leamon CP. Folate receptor expression in carcinomas and normal tissues determined by a quantitative radioligand binding assay. Anal Biochem. 2005;338:284–93.
2. Teng L, Xie J, Lee RJ. Clinical translation of folate receptor-targeted therapeutics. Expert Opin Drug Deliv. 2012;9:901–8.
3. Muller C, Schibli R. Folic acid conjugates for nuclear imaging of folate receptor-positive cancer. J Nucl Med : Off Publ Soc Nucl Med. 2011;52:1–4.
4. Salazar MD, Ratnam M. The folate receptor: what does it promise in tissue-targeted therapeutics? Cancer Metastasis Rev. 2007;26:141–52.
5. Ilgan S, Yang DJ, Higuchi T, Zareneyrizi F, Bayhan H, Yu D, et al. ^{99m}Tc-ethylenedicysteine-folate: a new tumor imaging agent. Synthesis, labeling and evaluation in animals. Cancer Biother Radiopharm. 1998;13:427–35.
6. Leamon CP, Parker MA, Vlahov IR, Xu LC, Reddy JA, Vetzel M, et al. Synthesis and biological evaluation of EC20: a new folate-derived, (99 m)Tc-based radiopharmaceutical. Bioconjug Chem. 2002;13:1200–10.
7. Fisher RE, Siegel BA, Edell SL, Oyesiku NM, Morgenstern DE, Messmann RA, et al. Exploratory study of ^{99m}Tc-EC20 imaging for identifying patients with folate receptor-positive solid tumors. J Nucl Med : Off Publ Soc Nucl Med. 2008;49:899–906.
8. Liu S, Edwards DS. ^{99m}Tc-labeled small peptides as diagnostic radiopharmaceuticals. Chem Rev. 1999;99:2235–68.
9. Leamon CP, Reddy JA, Dorton R, Bloomfield A, Emsweller K, Parker N, et al. Impact of high and low folate diets on tissue folate receptor levels and antitumor responses toward folate-drug conjugates. J Pharmacol Exp Ther. 2008;327:918–25.
10. Sirotnak FM, Tolner B. Carrier-mediated membrane transport of folates in mammalian cells. Annu Rev Nutr. 1999;19:91–122.
11. Qiu A, Jansen M, Sakaris A, Min SH, Chattopadhyay S, Tsai E, et al. Identification of an intestinal folate transporter and the molecular basis for hereditary folate malabsorption. Cell. 2006;127:917–28.
12. Zwicke GL, Mansoori GA, Jeffery CJ. Utilizing the folate receptor for active targeting of cancer nanotherapeutics. Nano Rev. 2012;3.

13. Matherly LH, Diop-Bove N, Goldman ID. Biological role, properties, and therapeutic applications of the reduced folate carrier (RFC-SLC19A1) and the proton-coupled folate transporter (PCFT-SLC46A1). 2011;1–34.
14. Antony AC. The biological chemistry of folate receptors. Blood. 1992;79:2807–20.
15. Shen F, Ross JF, Wang X, Ratnam M. Identification of a novel folate receptor, a truncated receptor, and receptor type beta in hematopoietic cells: cDNA cloning, expression, immunoreactivity, and tissue specificity. Biochemistry. 1994;33:1209–15.
16. Reddy JA, Xu LC, Parker N, Vetzel M, Leamon CP. Preclinical evaluation of (99 m)Tc-EC20 for imaging folate receptor-positive tumors. J Nucl Med : Off Publ Soc Nucl Med. 2004;45:857–66.
17. Leamon CP, DePrince RB, Hendren RW. Folate-mediated drug delivery: effect of alternative conjugation chemistry. J Drug Target. 1999;7:157–69.
18. Choi HS, Liu W, Misra P, Tanaka E, Zimmer JP, Itty Ipe B, et al. Renal clearance of quantum dots. Nat Biotechnol. 2007;25:1165–70.
19. Maurer AH, Elsinga P, Fanti S, Nguyen B, Oyen WJ, Weber WA. Imaging the folate receptor on cancer cells with ^{99m}Tc-etarfolatide: properties, clinical use, and future potential of folate receptor imaging. J Nucl Med : Off Publ Soc Nucl Med. 2014;55:701–4.